1 Hit and Track Finding

The BHF is a 2D hit reconstruction algorithm used in the electron lifetime analysis. The first step is to apply pedestal-subtraction and stuck ADC mitigation on the collection wire raw waveforms. Then, channel-by-channel, the waveform is copied to two parallel paths of processing. The first path begins with the application of a single-pole recursive filter with 6 sample decay time (-3 dB cutoff frequency of 53 kHz) [12] both forwards and backwards in the time domain to preserve the peak timing of the pulses. Following this, unipolar pulses are found when the amplitude of the filtered waveform raises above twice the measured noise RMS value. The start and end points of the pulse are fixed at -50 and +100 ticks, respectively, in relation to the tick at which the pulse is triggered. After all pulses on each waveform are detected, all combinations of pulses which have overlapping end and start values are merged. For each resulting "hit", the peak tick is calculated as the ADC-weighted mean tick between the start and end of the pulse. In this calculation, the weight function for tick i is $w_i = \exp(A_i - \sigma)/\sigma$, where A_i is the ADC value of tick i, and σ is the waveform noise RMS. The drift time for the hit is calculated as the peak time minus the detector trigger time. The hit charge is calculated on the unfiltered waveform in the second path of processing as the integral of ADC values between the start and end times as determined from the filtered waveform. Hit x coordinates are determined using the drift time and the detector drift velocity, and the z coordinates are simply the z location of the wire. The y coordinate of each hit was not measured directly as induction plane signals were not analysed, but could be roughly inferred through interpolation given the triggered muon counter x, y, and z locations.

The THB algorithm was developed to purify the hits collection output of the BHF. In addition to real hits, the high noise on raw waveforms causes many fake hits to be created which do not correspond to any real particle track or shower. The THB begins by masking out BHF hits which are further than 25 cm perpendicular distance from the line which connects the two triggered muon counters in $x - z$ space, outside of the counter shadow. The hits which pass this cut are subject to a robust polynomial fitting process, based on the MLESAC algorithm [1]. The algorithm fits a random subsample of the event hits to a quadratic polynomial model (small curvatures are allowed in the track to account for the effects of field non-uniformities on drifting charge, in particular, caused by space charge), then calculates the negative log likelihood which weights hits within a threshold perpendicular distance of the best-fit model based on this distance, and weights outliers zero. The process is repeated over many subsamples of hits until the minimum negative log likelihood is found within a fixed number of iterations. The final step in the THB is to overlay the track in wire-time space onto all of the collection plane waveforms. If the wire signal did not raise above the hit finding threshold in the BHF on any non-bad wire at the time where the track predicts a hit should exist, a charge deposit is assumed at that time and location. For these assumed hits, the start and end times are interpolated using hits found by the BHF on neighbouring wires, and the hit peak time and charge are calculated in exactly the same way as the hits found in the BHF. A pseudo-3D reconstruction of the track in the detector is created by using the z and x coordinates of the hits, and roughly estimating the y coordinate by using the triggered muon counter locations. The track angles with respect to the anode plane are also estimated by using the 3D line which connects the triggered muon counters.

2 Electron Lifetime Measurement

Complementary to the dedicated purity monitors, the electron lifetime of the liquid argon was studied using cosmic muon tracks in the TPC. Such a measurement is important in quantifying and correcting for the overall effect of impurities inside the TPC on the drifting ionization

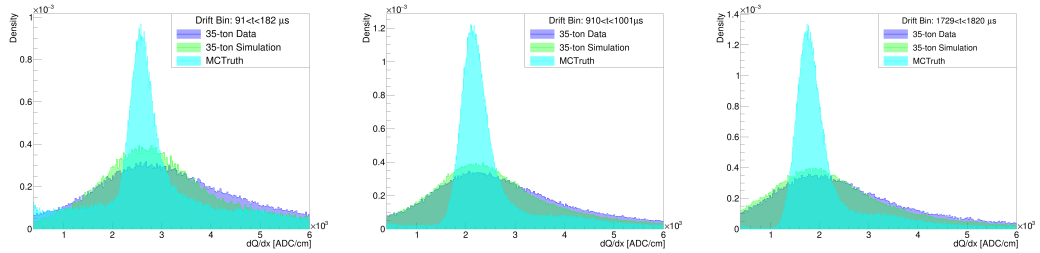

(a) Short Drift ($91 < t_{drift} < 182$ μs)

(b) Medium Drift ($910 < t_{drift} < 1001$ μs)

(c) Long Drift ($1729 < t_{drift} < 1820$ μs)

Figure 1: dQ/dx from reconstructed 35-ton data, simulation, and MC truth.

charge. Free electrons in the LAr attach to electronegative impurities (such as oxygen and water), effectively reducing their drift velocity to zero, thereby reducing the total charge collected at the anode. For example, a reduction of 20% in charge collected, versus total charge liberated in an interaction, for a drift of 2 m and electric field of 500 V/cm is expected for an electron lifetime of 20 ms [8]. Measuring the electron lifetime with a high accuracy is therefore required for the next generation of massive liquid argon TPCs, such as DUNE. Several experiments have successfully measured the electron lifetime using methods similar to the one described here [4, 3, 5, 6, 7].

The electron lifetime is defined by the exponential decay of the collected charge with drift time,

$$Q_{\mathrm{c}} = Q_0 e^{-t/\tau}, \tag{1}$$

where Q_{c} is the collected charge at the anode, Q_0 is the charge liberated in the ionization, t is the drift time, and τ is the electron lifetime.

In this analysis, hits associated with successfully reconstructed tracks from the THB 1 are used to determine the lifetime. Because of the Landau fluctuations in energy loss by minimally ionizing particles, the collected hit charge on the readout wires follows a Landau distribution, and the electron lifetime is determined by the decay of the most probable value (MPV) of the distribution as a function of drift time. To account for varying track angles with respect to the anode plane, the hit charge on each wire is divided by the factor $p/\cos\theta$ where p is the collection wire spacing and θ is the angle between the track and the vector perpendicular to the collection wire and in the plane of wires. The resulting aggregations of normalized hit charges (dQ/dx) are divided into 22 drift time bins, each of width ~91.5 μs (~10 cm given the drift velocity) based on the hit drift times as calculated by the BHF (section 1). Three examples of bins of dQ/dx are shown in figure 1. In each bin, the data are fit to a Landau convoluted with a Gaussian representing the detector response. The range for these fits is chosen to be narrow such that the expected delta electron peak above the muon ionization Landau, and the low-charge hits with low efficiency and poor resolution, are excluded while retaining the Landau peak. The extracted Landau MPVs from the fits are then plotted against mean drift time for the bin, and the lifetime determined from an exponential fit as in equation 1.

The data used in this analysis consists of 20,244 events, triggered on East-West crossing muons, from seven non-consecutive days of the Phase II run when the cathode HV was stable, the PrMs reported greater than 2 ms lifetime, and the detector was in the low noise state. Fluctuations in the electron lifetime over the course of the run and throughout the entire TPC volume are not studied in this analysis, but are measured by the PrMs to vary by approximately 9% over the course of this data set. As measured by PrM2, the mean lifetime in the cryostat

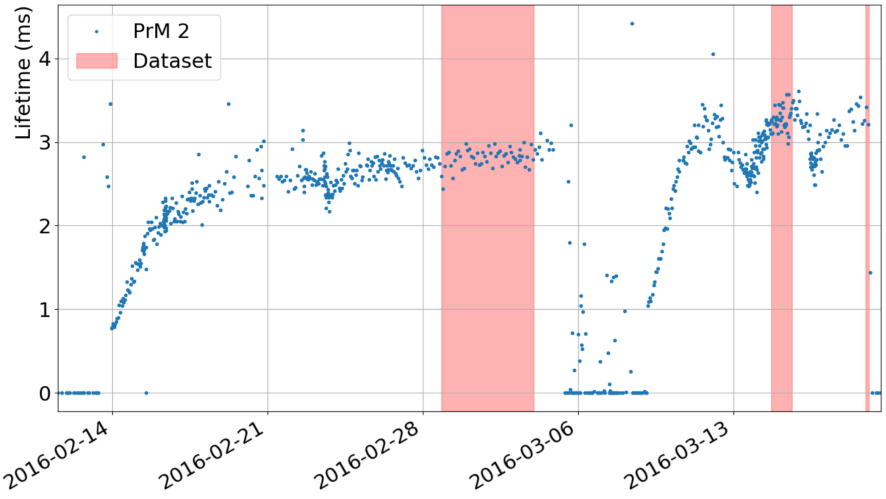

Figure 2: PrM 2 measured electron lifetimes over the course of the 35-ton Phase II run. The times during which the datasets in this analysis were recorded are shown in shaded red regions.

but outside of the TPC for this dataset is 3.0 ± 0.3 (stat.) ± 0.5 (syst.) ms, as in figure 2.

For this data set, the decay of hit dQ/dx in the TPC is shown in figure 3, yielding an observed electron lifetime of 4.53 ± 0.10 (stat.) ms (systematic uncertainties and corrections to this measurement are made in section 2.2). Here, a fiducial cut of 50% of the full drift time is imposed to reduce bias due to incorrectly determined MPV for longer drift hits (explanation in section 2.1.4). Possible causes of bias in this measurement and explanation of the systematic uncertainties are described below.

2.1 Examining the bias through simulations

The signal-to-noise ratio (S/N) and particular electronic noise characteristics of the 35-ton are hypothesized to be the most significant factors influencing the bias in the electron lifetime measurement. Phenomena such as the varying noise frequency spectrum across the whole data-taking run, the varying noise amplitudes across the run as well as across channels, and the coherent noise between channels with the same voltage regulator are not included in the standard Monte Carlo simulation of the detector. Therefore, to accurately reflect the 35-ton noise characteristics, a data-driven noise model was devised for the simulation which uses real 35-ton data waveforms to define the noise.

2.1.1 Data-Driven Noise Simulation

The simulation uses CRY [2] to generate a single muon per event in the 35-ton geometry using the provided muon direction and energy flux parameterisations. Events where the muon passes through an East-West counter trigger pair are kept and propagated through the Geant4 step in the normal LArSoft simulation [**?**]. The detector simulation of the event occurs without addition of the simulated electronic noise. The noiseless simulated wire signals are passed to the separate noise simulation step.

This process combines the simulated noiseless waveforms with representative data noise waveforms. The data noise waveforms are taken from real 35-ton data events, from the same data set as described in section 2. To remove the impact of triggered particle signals in the data

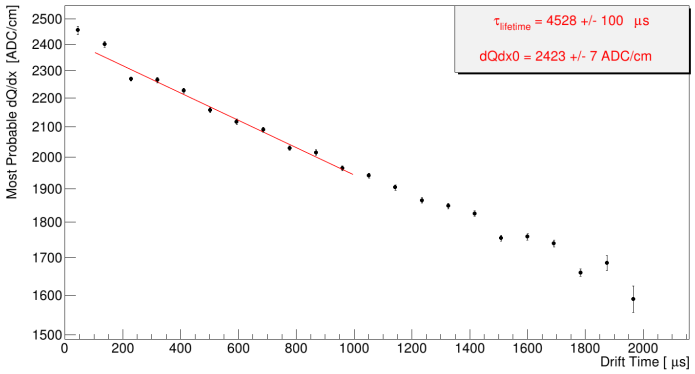

Figure 3: Most probable hit dQ/dx measured at the anode, as a function of drift time. Exponential fit to fiducial range shown in red.

waveforms, smaller unbiased sub-slices of the data waveforms are used: the final 5200 ticks of each 15000 tick waveform (see section **??**) are guaranteed to be free of triggered particle signals as the negative ionization charge will have already drifted to the anode. Remaining un-triggered particle signals in the data waveforms are kept as representative real backgrounds. Furthermore, missing or dead channels in the data sample are not propagated through the simulation, accurately reflecting the varying run characteristics of the 35-ton detector.

The two source waveforms are combined by a scaled ADC-by-ADC addition. In order to simulate the effects of different possible levels of S/N, the simulated signal waveforms may be scaled by a factor, "MCscale", which represents a relative multiplier on the true S/N of 35-ton data. For example, MCscale=2.0 represents twice the S/N of the 35-ton data, or in other words, half as much noise.

Following the data-driven noise simulation, the BHF and THB are used to reconstruct hits and tracks and the electron lifetime analysis proceeds using exactly the same procedure as for real 35-ton data.

80 simulated datasets are created using the process described here, each with the same initial ~35,000 East-West triggered simulated cosmic muon events. Five electron lifetimes are simulated (2.5 ms, 3.0 ms, 3.5 ms, 4.0 ms, and 4.5 ms), and for each lifetime, 16 different S/N scale factors are simulated, ranging from 0.5 to 2.0 in increments of 0.1.

2.1.2 Hit Reconstruction Purity and Efficiency

The performance of the BHF and THB on real and simulated data is summarised by the efficiency and purity statistics. In each simulated event, the reconstructed hit times are compared with the Monte Carlo truth information from the simulation to determine which reconstructed hits are "true". Efficiency, ϵ_S, is then defined as the number of reconstructed hits with matching MC truth hits divided by the total number of MC truth hits. Purity, ϕ, is defined as the number of MC-matched reconstructed hits divided by the total number of reconstructed hits. For the simulations, the hit finding efficiency and purity are calculated as functions of drift distance, as in figure 4, and as functions of MCscale, as in figure 5. The purity of reconstruction is high (>94%) for all simulated datasets, even if the simulated noise is higher than the 35-ton noise. Thus, it can be said that if a hit is found, then it is highly likely to be a real hit, a direct consequence of the robust MLESAC algorithm implementation described in section **??**. Similarly, the efficiency

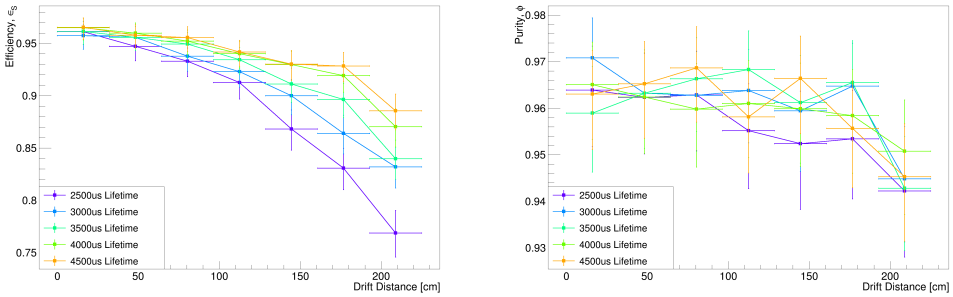

Figure 4: Efficiency (left) and purity (right) of hit finding as functions of drift distance for several values of electron lifetime.

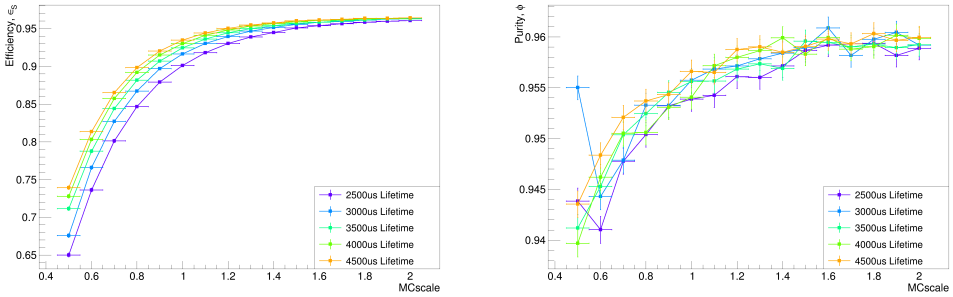

Figure 5: Efficiency (left) and purity (right) of hit finding as functions of MCscale parameter for several values of electron lifetime.

is high for hits near the anode and in the presence of low detector noise, but drops significantly for longer drifts and high noise. Because of impurities, the hit charge is attenuated over the full drift length to below the hit finding threshold, thereby reducing the efficiency, despite the assumption of hit locations based on neighboring large charge hits in the BHF.

The dependence of efficiency on drift distance is a motive to apply a fiducial cut on the sensitive region of the TPC, nearer to the APA. The steep drop in efficiency for detectors with higher noise than the 35-ton (lower MCscale parameter) reinforces the necessity for low-noise readout in order to efficiently and accurately reconstruct events.

2.1.3 Hit Charge Efficiency and Resolution

Independent of electron lifetime, the hit finding efficiency versus MC hit charge illustrates the main source of bias in the analysis. As in figure 6, the efficiency drops to zero for decreasing charge deposits, as the smaller charge hits fall below the threshold for detection. Because the distribution of hit finding thresholds on all wires is variable dependent on noise level, the actual efficiency resembles a sigmoid function with 50% cutoff which depends on the S/N. This shape of efficiencies has major implications on the measurement of the most probable dQ/dx. For example, an illustration of the effect of a sigmoid threshold function on a Landau curve is shown in figure 7. As the Landau MPV shifts down due to charge attenuation over drift, the distribution impresses upon the threshold, and causes the apparent MPV to stagnate, even though the true

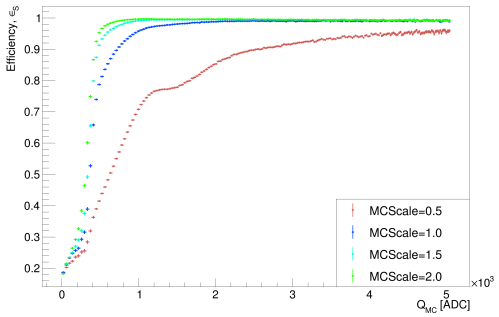

Figure 6: Hit finding efficiency vs. hit charge for several values of MCscale parameter. Coloured bands represent spread of values (standard deviation), error bars represent standard error on the mean.

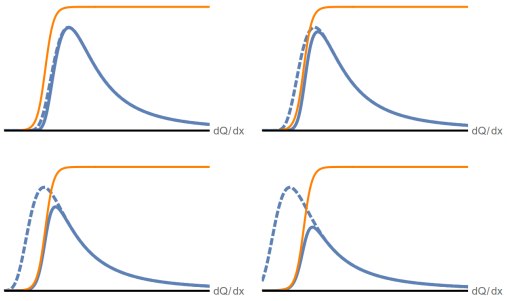

Figure 7: Hypothetical effect of sigmoid threshold on Landau function. The dashed function represents the un-cut Landau.

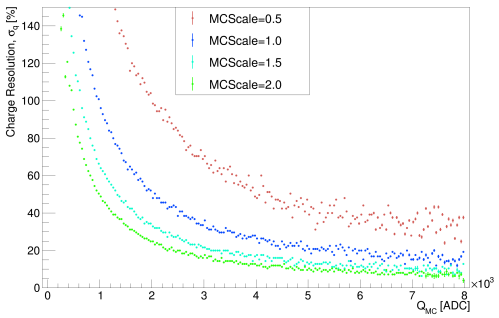

Figure 8: Charge resolution vs. hit charge for simulated data.

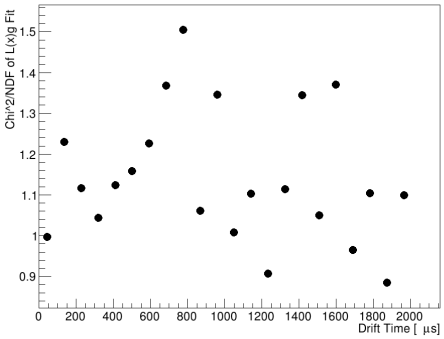

Figure 9: Fit χ^2/N.D.F. for Landau $\otimes$ Gaussian fits.

MPV continues to decrease. This then biases the observed lifetime toward higher values, away from the true lifetime. This effect is expected to account for the majority of the difference between the observed lifetime from this analysis and the observed lifetime from the PrM system.

Figure 8 shows the charge resolution, σ_q, defined as the FWHM of the standardised charge residual distribution, $(Q_{MC} - Q_{Reco})/Q_{MC}$, as a function of hit charge. The varying resolution across the range of hit charges relevant to the lifetime analysis implies a modified detector Gaussian resolution function where the width parameter is a function of hit charge. This alternative parameterisation of the Landau-Gaussian convolution fit function is not studied here, instead it is assumed as part of the systematic uncertainty in the current analysis. Despite these potential model-dependent differences, the freedom allowed the Landau$\otimes$Gauss parameters is sufficient to maintain good fits across all drift bins, as evidenced by the χ^2/N.D.F. values in figure 9. Therefore, these systematics are expected to be less important than the overall charge-dependent bias imposed by the threshold effect as described above.

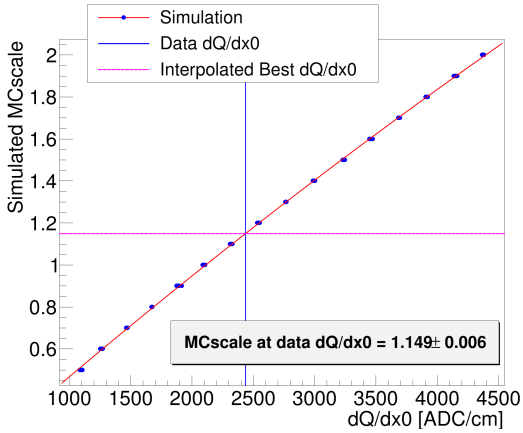

Figure 10: Exponential fit dQ/dx_0 parameter for all simulated datasets. Blue dashed line represents the true data dQ/dx_0 value, and the true MCscale parameter is determined through interpolation.

2.1.4 Fiducial Cut

The fact that the bias between the true MPV and the observed MPV increases with drift distance motivates a fiducial cut for the lifetime measurement. Defining a threshold for this cut, however, is not possible without prior knowledge of the true lifetime. Nevertheless, it is known that there is *less* bias in the measured hit charges with shorter drift times (near the anode) than with longer drift times (near the cathode). Based on this observation, an arbitrary fiducial cut of 1/2 the full drift time is imposed to reduce the bias on the electron lifetime measurement. Stricter cuts are hypothesized to reduce the bias even further, but this dependence (and the effects on overall measurement uncertainties) is not studied. To illustrate the effectiveness of the 50% cut, the measured lifetime from the full detector drift distance is observed as 4.93 ± 0.05 ms, compared with 4.53 ± 0.10 ms with the 50% cut imposed (see figure 3). A drift distance dependent bias clearly exists, and is attributed to the decreasing hit efficiency and worsening charge resolution at longer drift lengths. Quantifying this bias is done by comparing the lifetimes extracted from the simulated data sets to the true simulated lifetime.

2.1.5 Signal Simulation Scaling

While all aspects of the 35-ton electronic noise are directly reproduced in the simulation, uncertainty remains in the collection wire signal simulation. The most probable charge deposited in the TPC in the absence of charge attenuation due to impurities is given by the intercept parameter in the exponential fit (equation 1), dQ/dx_0. Comparison of dQ/dx_0 between 35-ton data and all simulated datasets reveals that the simulation with MCscale=1 does not accurately model the true S/N of 35-ton data (figure **??**). Instead, scaling up the amplitude of signal simulation by an additional 15% more closely reproduces the 35-ton data, though further study of the causes of these differences is not pursued. This bias is mitigated by using the simulated data sets with MCscale parameter of 1.1 (or 1.2), allowing more accurate comparisons between datasets. The remaining differences between simulation and 35-ton data are included in the overall estimation of systematic uncertainty.

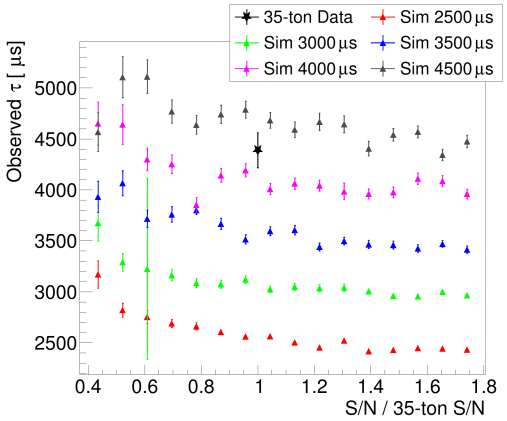

Figure 11: Measured electron lifetime of simulated data and 35-ton data. Dashed lines indicate true lifetime for simulated data sets.

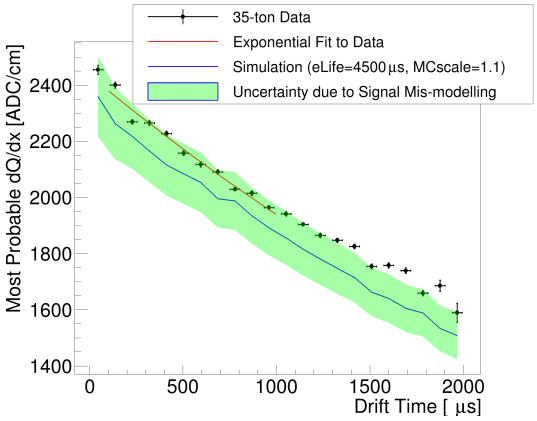

Figure 12: Data dQ/dx MPV (black) overlaid with most similar simulated dQ/dx MPV (blue). Green band represents the uncertainty due to MCscale parameter.

2.2 Debiasing the Electron Lifetime

By analyzing the electron lifetime of many simulated datasets of varying parameters and comparing the results with the measured data, the lifetime of the 35-ton data set can be extracted. Figure 11 shows the true simulated lifetimes (dashed lines) and the observed lifetimes (plot points), as a function of noise level. For simulated datasets, the horizontal scale is MCscale/1.149, correcting for signal simulation error. The bias in the observed lifetime for higher noise can be seen for lower MCscale values, a result of the drift-dependent upward bias in Landau MPVs. The measured lifetime for the 35-ton data is consistent with the 4.0 ms and the 4.5 ms lifetime simulations, and the nearest MCscale parameter of 1.1, confirmed in figure 12. More precise determination of the true electron lifetime of the 35-ton data is done by interpolation.

The true (debiased) data electron lifetime is determined by performing a multivariate linear regression on the simulated dataset results using the function

$$\tau_{\mathrm{true},i} = a_0 + a_1 \mathrm{S}_i + a_2 \tau_{\mathrm{o},i} + a_3 \mathrm{S}_i \tau_{\mathrm{o},i} + a_4 \mathrm{S}_i^2 + a_5 \tau_{\mathrm{o},i}^2$$

for $i = 1...n$ datasets where τ_{true} is the simulated electron lifetime, τ_{o} is the observed electron lifetime, and S=MCscale/1.149 is the reduced simulated MCscale parameter, relative to the data MCscale parameter. Evaluation of the least squares regression model reveals that for data (S=1.0, $\tau_o = 4.53 \pm 0.10$ ms), the true lifetime is $\tau_{\mathrm{true}} = 4.25 \pm 0.24$ ms.

2.3 Systematic Uncertainties

The magnitude of the total systematic uncertainty is taken as the absolute difference between the observed lifetime and the inferred lifetime as determined by comparing with simulations. This difference is large enough to account for the most significant biases which affect the simulation and the data in the same way, including channel-by-channel differences in signal scaling in the simulation, efficiency losses due to high hit finding threshold, poor charge resolution of low-charge hits, and space charge distortions in the electric field. Other differences between data and simulation are second order and expected to contribute much less to the overall systematics.

Therefore, $4.53 - 4.25 = 0.28$ ms is taken as the overall systematic uncertainty as a result of the biases which were not able to be individually studied and quantified.

The measured lifetime of 4.25 ± 0.24 (stat.) ± 0.28 (syst.) ms is somewhat consistent with the average of the purity monitor measurements, 3.0 ± 0.2 (stat.) ± 0.5 (syst.) ms, over the same span of runs. The difference may be explained by inefficient mixing of impurities throughout the full cryostat volume. Previous internal computational fluid dynamics studies of the impurity mixing in the cryostat, taking into account fluid flow through the TPC field cage, suggest the possibility of at least a 10% difference in the overall impurity concentration between the location of PrM2 and within the TPC field cage [9].

Further differences may be attributed to the accumulation of positive space charge in the TPC, which, because of their low mobility in comparison to the negative drift electrons, distorts the electric field [10]. Based on the nominal drift field of E_0=250 V/cm, the full drift distance of 2.2 m, and the rate of creation of positive ion density due to cosmic ray muons at the surface of the earth of about 1.8×10^{-10} C/m^3/s, the actual electric field becomes $0.89E_0$ at the anode, and $1.19E_0$ at the cathode. This overall field non-uniformity affects the probability of a drift electron to recombine with an argon ion. According to [11], the fraction of ionization electrons from a 1.8 MeV muon which survive recombination is 64.3% in the absence of space charge, and 62.5% at the anode and 66.7% at the cathode with space charge distortions. This means a 4.2% difference in available charge for drifting between the anode and cathode as a result of recombination alone. By equating two exponential decay functions $e^{-t/\tau}$ and $e^{-t/\tau'}$, while imposing the requirements that the functions must be equal-valued at $t = 0$ and must differ by 4.2% at $t = T$, we recover a formula for the lifetime parameter adjusted for space charge, τ', as a function of α which represents the difference in recombination coefficients from $t = T$ to $t = 0$,

$$\tau'(\alpha) = \frac{T\tau}{T + \tau \log(1 + \alpha)}.$$

Thus, for this analysis ($\tau = 4.25$ ms and $T \approx 2$ ms), the expected contribution of space charge distortions in electric field to the total systematic uncertainty of the electron lifetime to be 2.9% for the fiducial region described in section 2.1.4, which accounts for nearly half of the total 6.6% systematic uncertainty of this analysis.

References

[1] P. H. S. Torr and A. Zisserman, "MLESAC: A new robust estimator with application to estimating image geometry". Computer Vision and Image Understanding. 78(1), 138-156. doi:10.1006/cviu.1999.0832 (1996).

[2] C. Hagmann, D. Lange, and D. Wright, "Cosmic-ray shower generator (CRY) for Monte Carlo transport codes". 2007 IEEE Nuclear Science Symposium Conference Record. 2, 1143 (2007).

[3] arXiv:0910.5087v2

[4] Amoruso, S., et al. (2004). "Analysis of the liquid argon purity in the ICARUS T600 TPC". Nucl. Instrum. Meth. A **516**, 68-79.

[5] M. Antonello *et al.*, "Experimental observation of an extremely high electron lifetime with the ICARUS-T600 LAr-TPC," JINST **9**, no. 12, P12006 (2014) doi:10.1088/1748-0221/9/12/P12006 [arXiv:1409.5592 [physics.ins-det]].

[6] Anderson, C., et al. (2012). "The ArgoNeuT detector in the NuMI low-energy beam line at Fermilab". JINST **7**, P10019. arXiv:1205.6747

[7] Bromberg, C., et al. (2015). "Design and operation of LongBo: a 2 m long drift liquid argon TPC", JINST **10**, no. 07, P07015 (2015).

[8] baibussinov jinst 5 P03005

[9] Michna, G. J., Gent, S. P., and Propst, A. (2017). "CFD Analysis of Fluid, Heat, and Impurity Flows in DUNE FAR Detector to Address Additional Design Considerations", DUNE DocDB 3213.

[10] Palestini, S., et al., "Space charge in ionization detectors and the NA48 electromagnetic calorimeter", Nucl. Instr. and Meth. A **421**, 75 (1999).

[11] Acciarri, R., et al. "A study of electron recombination using highly ionizing particles in the ArgoNeuT Liquid Argon TPC". JINST **8**, P08005 (2013).

[12] Smith, S. W. "The Scientist and Engineer's Guide to Digital Signal Processing". California Technical Publishing, San Diego, CA, (1997). ISBN:0-9660176-3-3.